

## Supporting Information

### Investigation of non-precious metal cathode catalysts for direct borohydride fuel cells

*Yu Guo,<sup>a</sup> Yingjian Cao,<sup>a</sup> Qinggang Tan,<sup>b</sup> Daijun Yang,<sup>a</sup> Yong Che,<sup>c</sup> Cunman Zhang,<sup>a</sup>  
Pingwen Ming,<sup>a</sup> and Qiangfeng Xiao<sup>a\*</sup>*

---

<sup>a</sup>School of Automotive Studies & Clean Energy Automotive Engineering Center,  
Tongji University (Jiading Campus), 4800 Cao'an Road, Shanghai 201804, China

<sup>b</sup>School of Materials Science & Engineering, Tongji University (Jiading Campus),  
4800 Cao'an Road, Shanghai, 201804, China

<sup>c</sup>Enpower Beijing Corp. 13 Area 2 Jinsheng Street, Daxing, Beijing, 06500

\*Corresponding Authors. E-mail: xiaoqf@tongji.edu.cn (Q.X.).

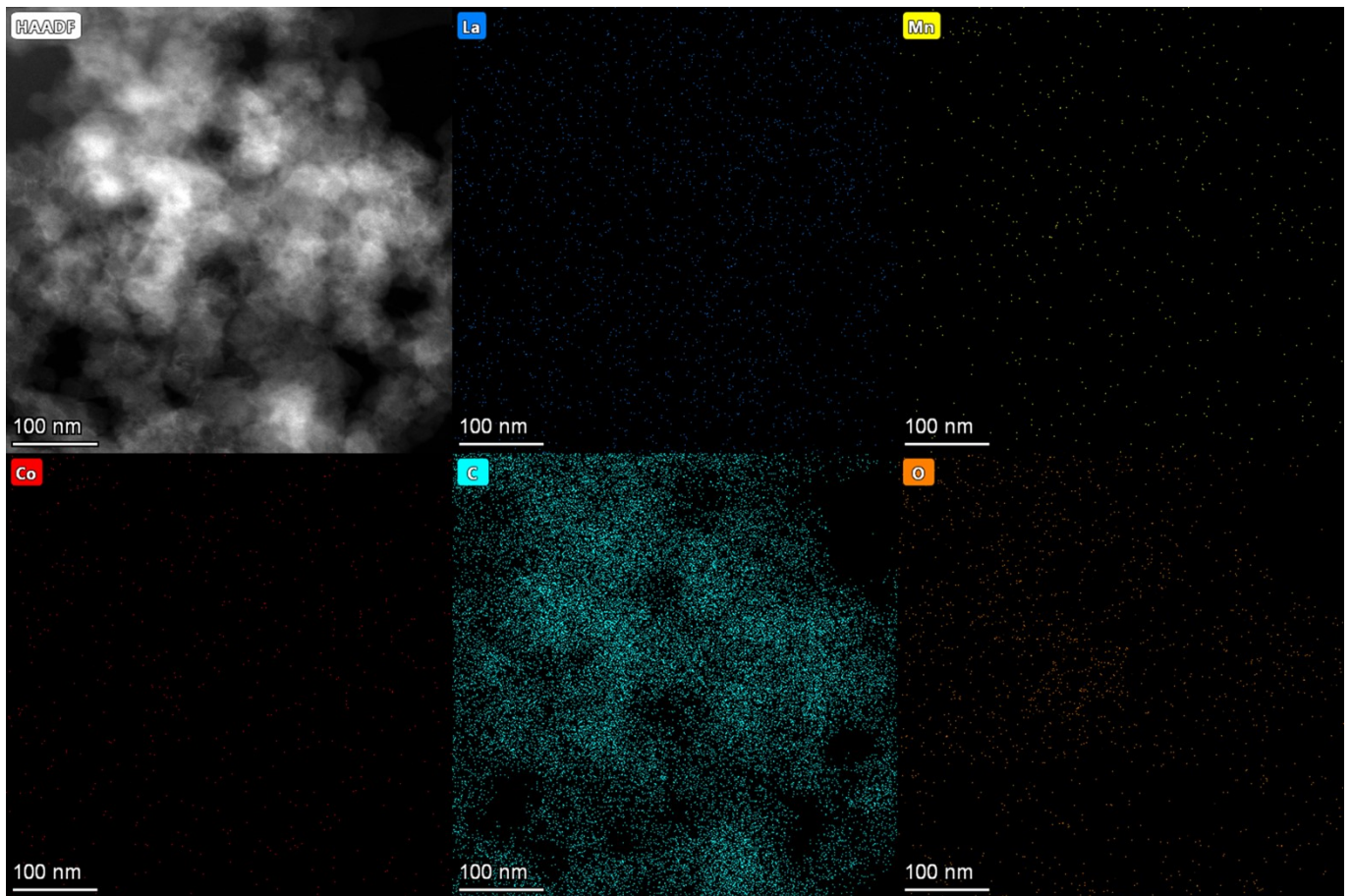


**Figure S1.** HAADF-TEM and EDS elemental mapping image of pristine LMCO electrode.

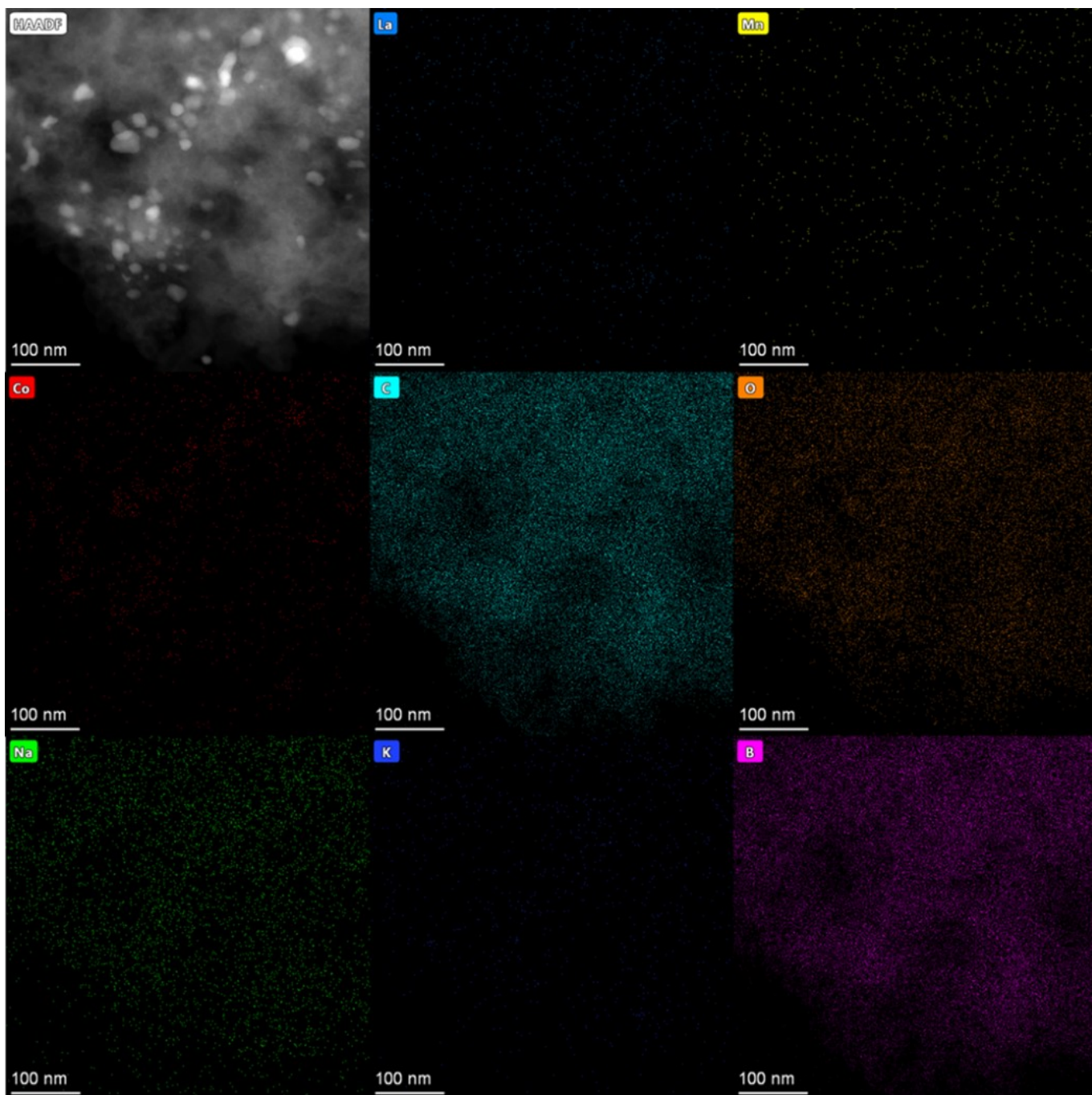


**Figure S2.** HAADF-TEM and EDS elemental mapping image of LMCO electrode after durability test.

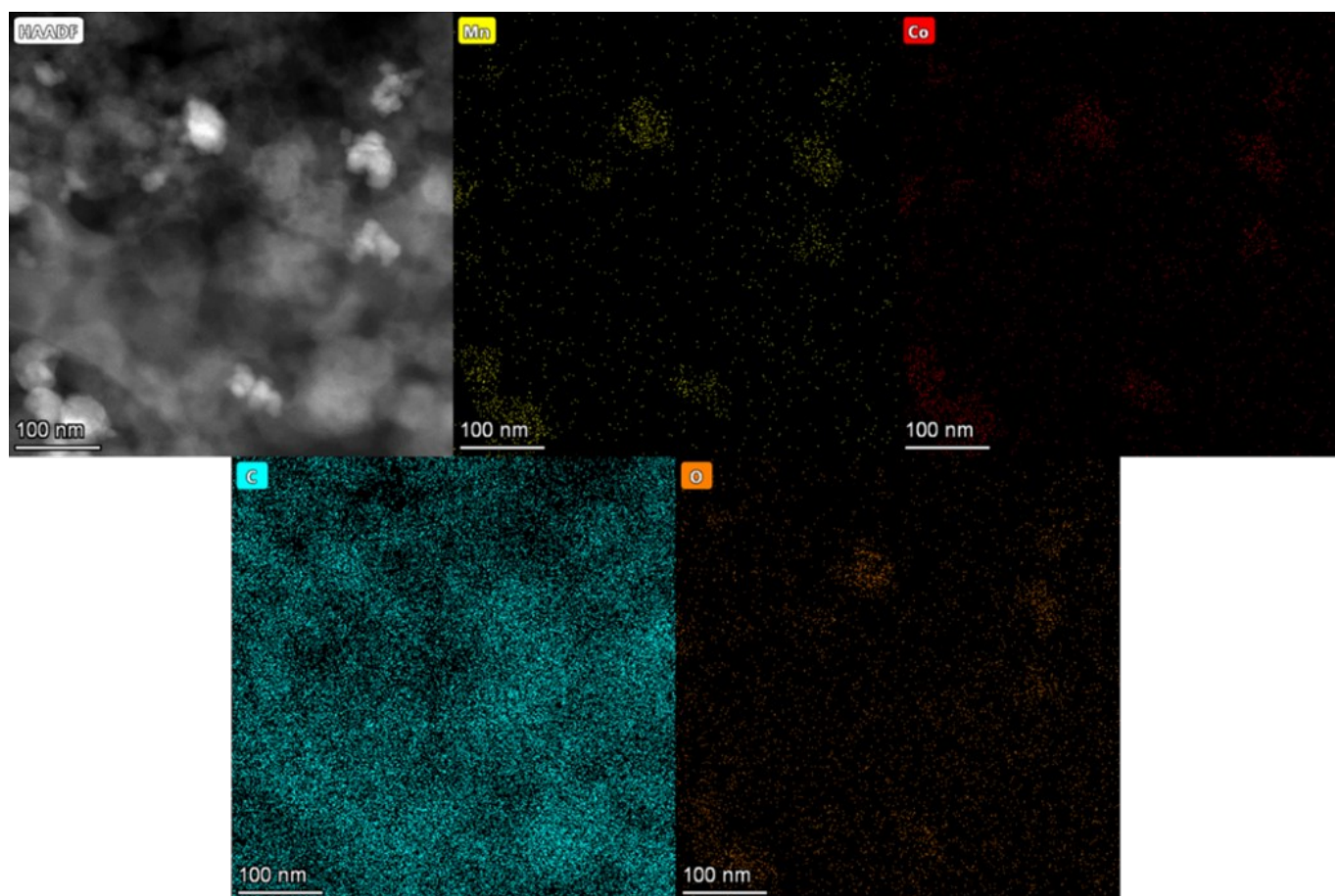


**Figure S3.** HAADF-TEM and EDS elemental mapping image of pristine MCS electrode.



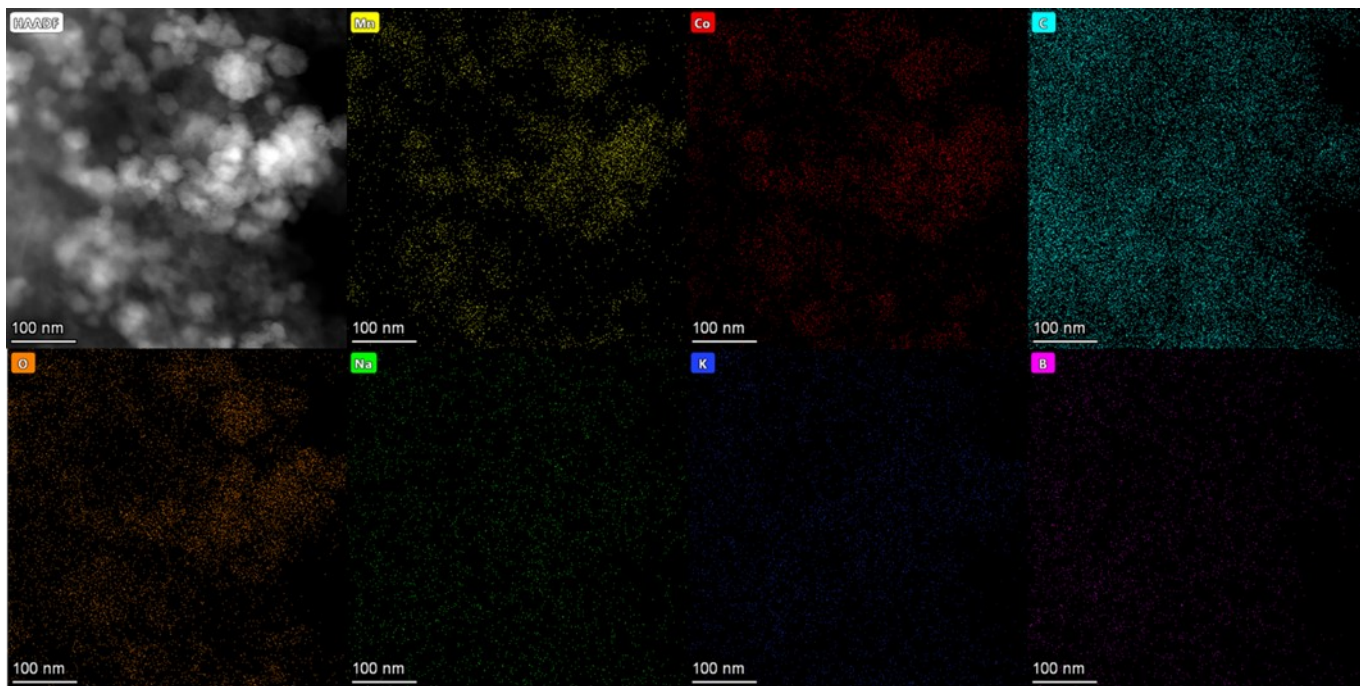


**Figure S4.** HAADF-TEM and EDS elemental mapping image of MCS electrode after durability test.

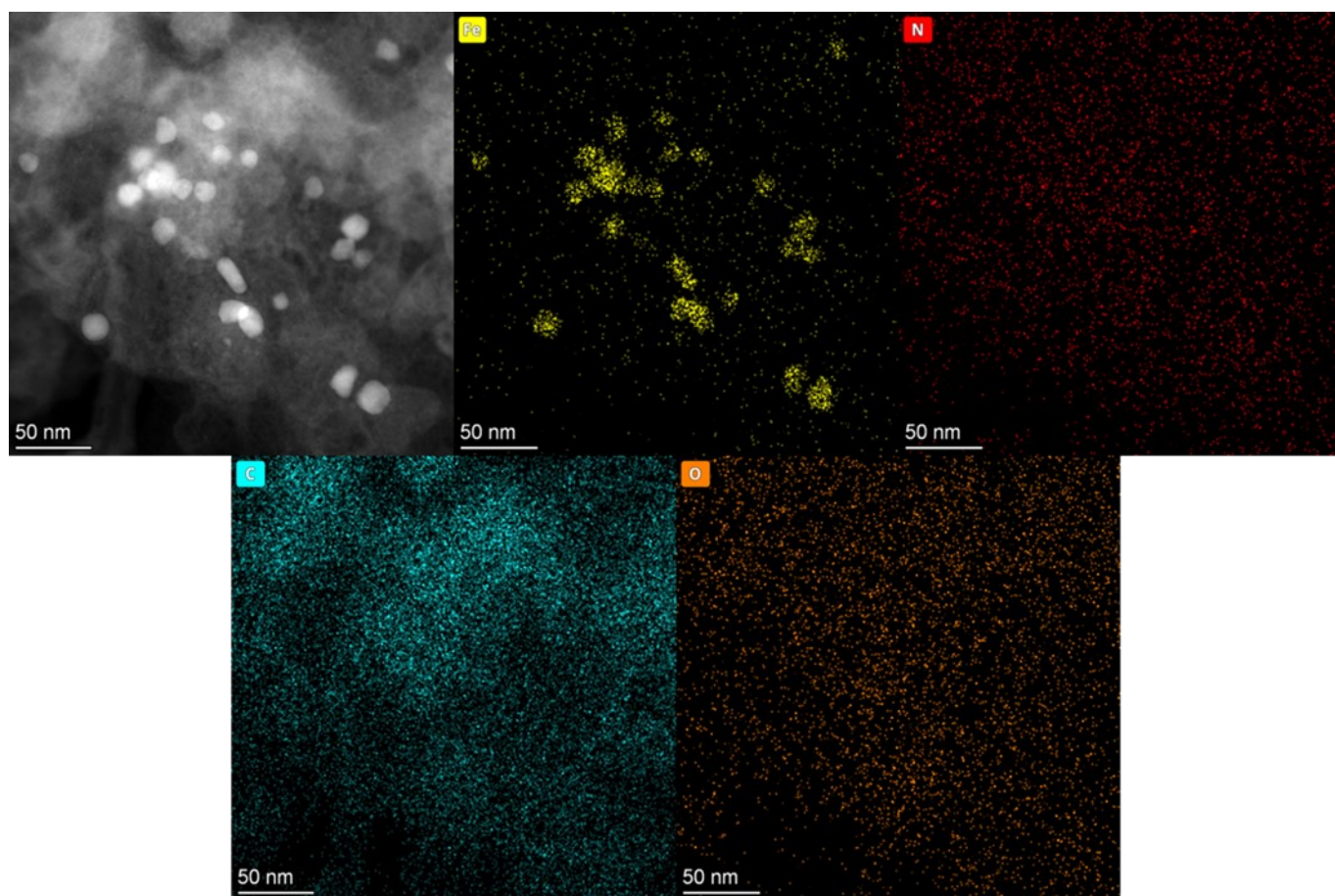


**Figure S5.** HAADF-TEM and EDS elemental mapping image of pristine Fe-N-C electrode.

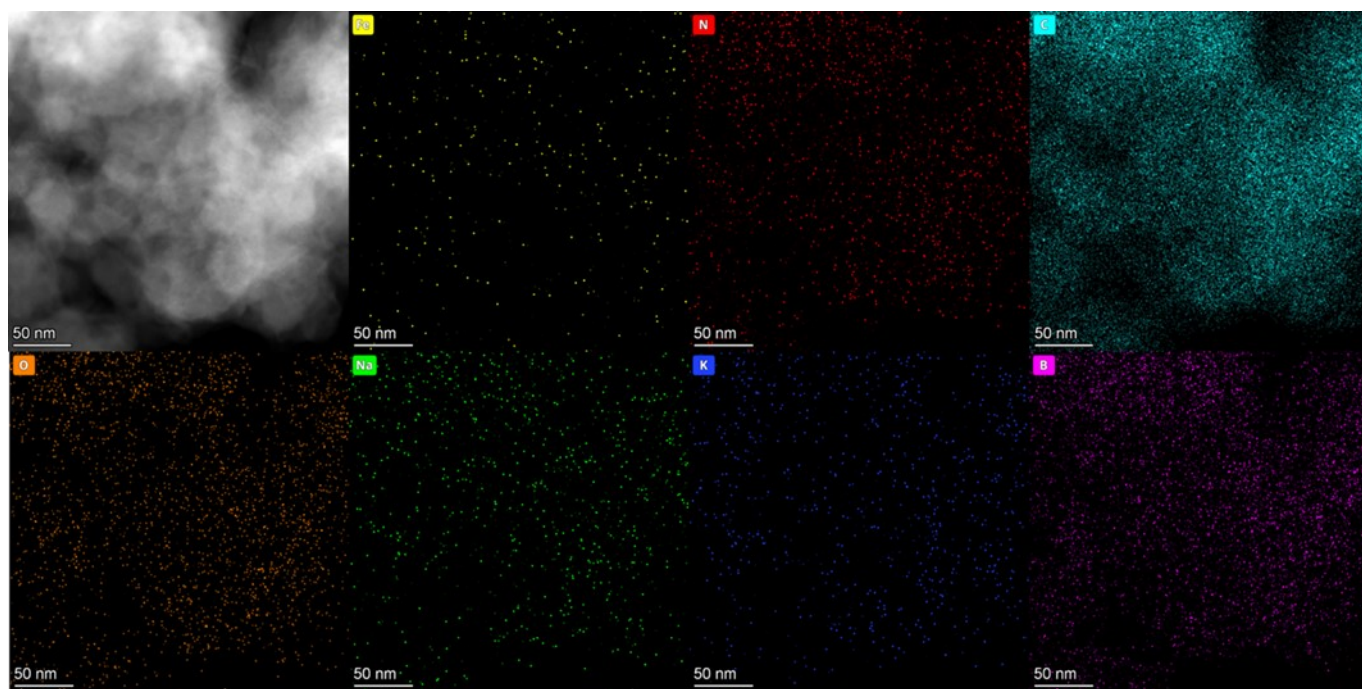


**Figure S6.** HAADF-TEM and EDS elemental mapping image of Fe-N-C electrode after durability test.

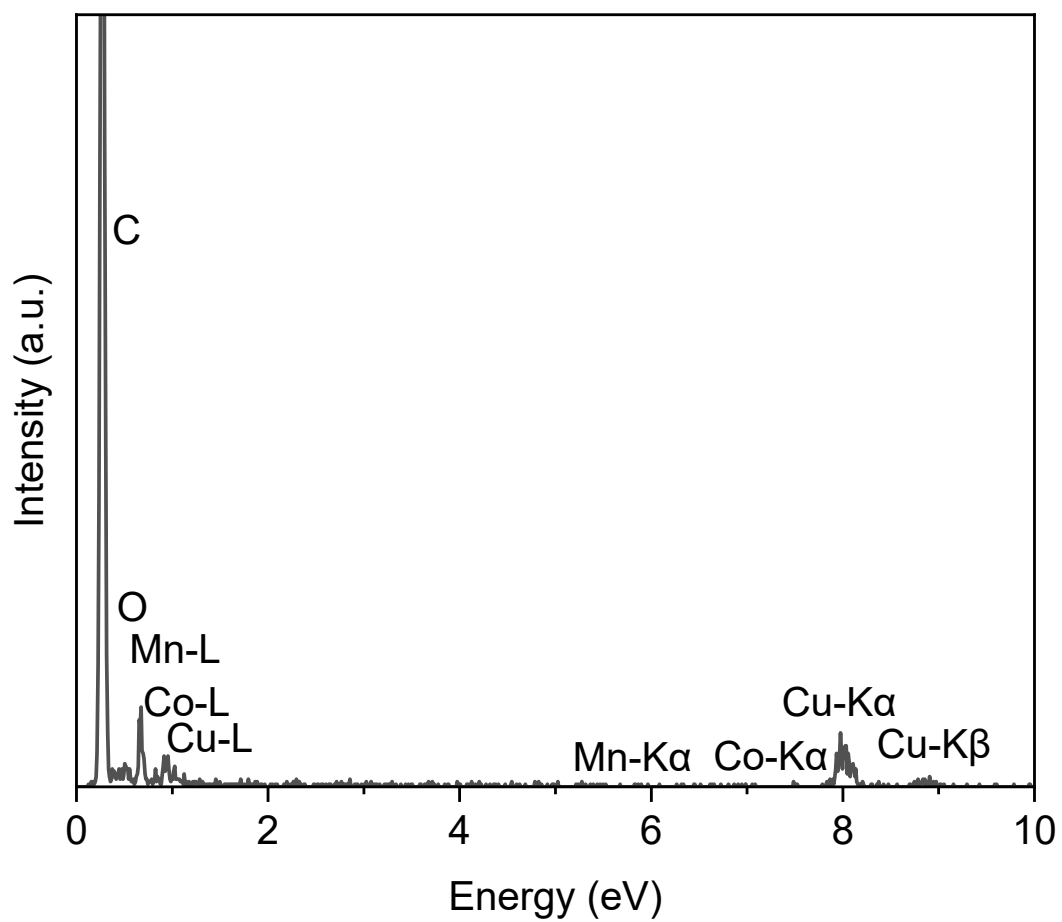


**Figure S7.** EDS elemental spectrum of pristine LMCO electrode.



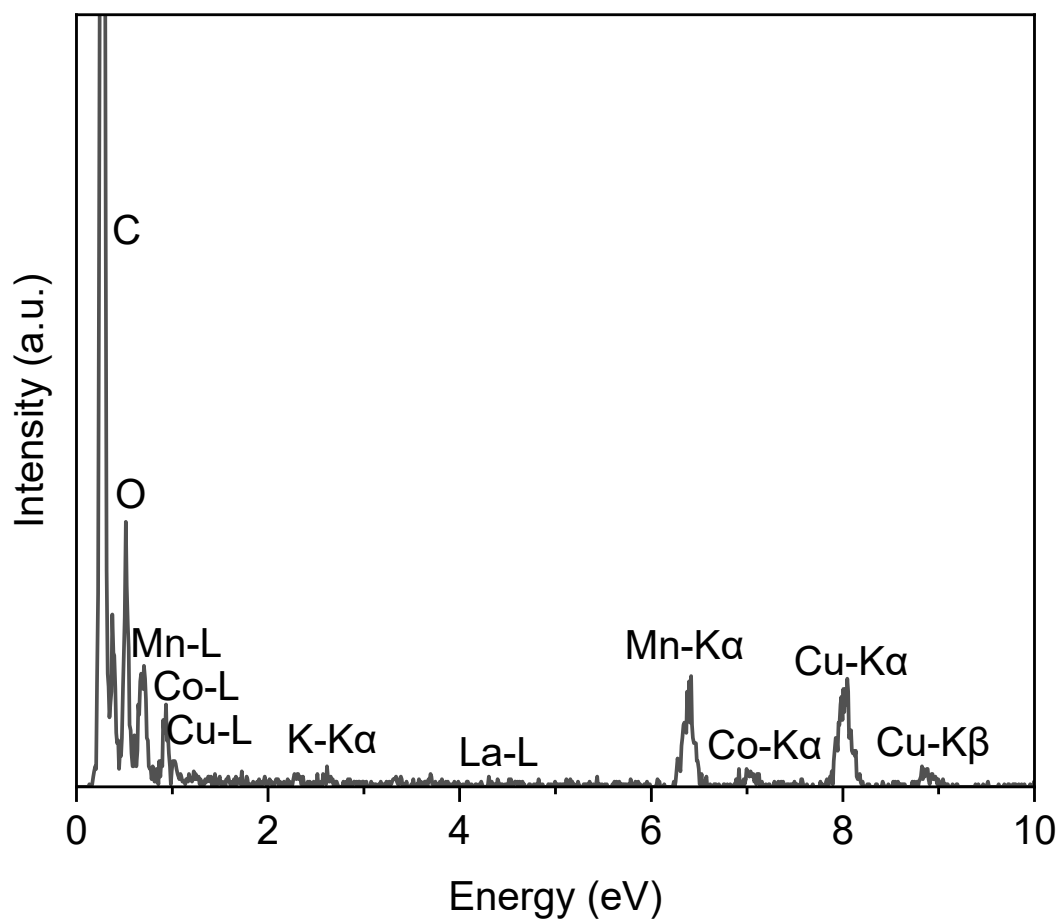


**Figure S8.** EDS elemental spectrum of LMCO electrode after durability test.

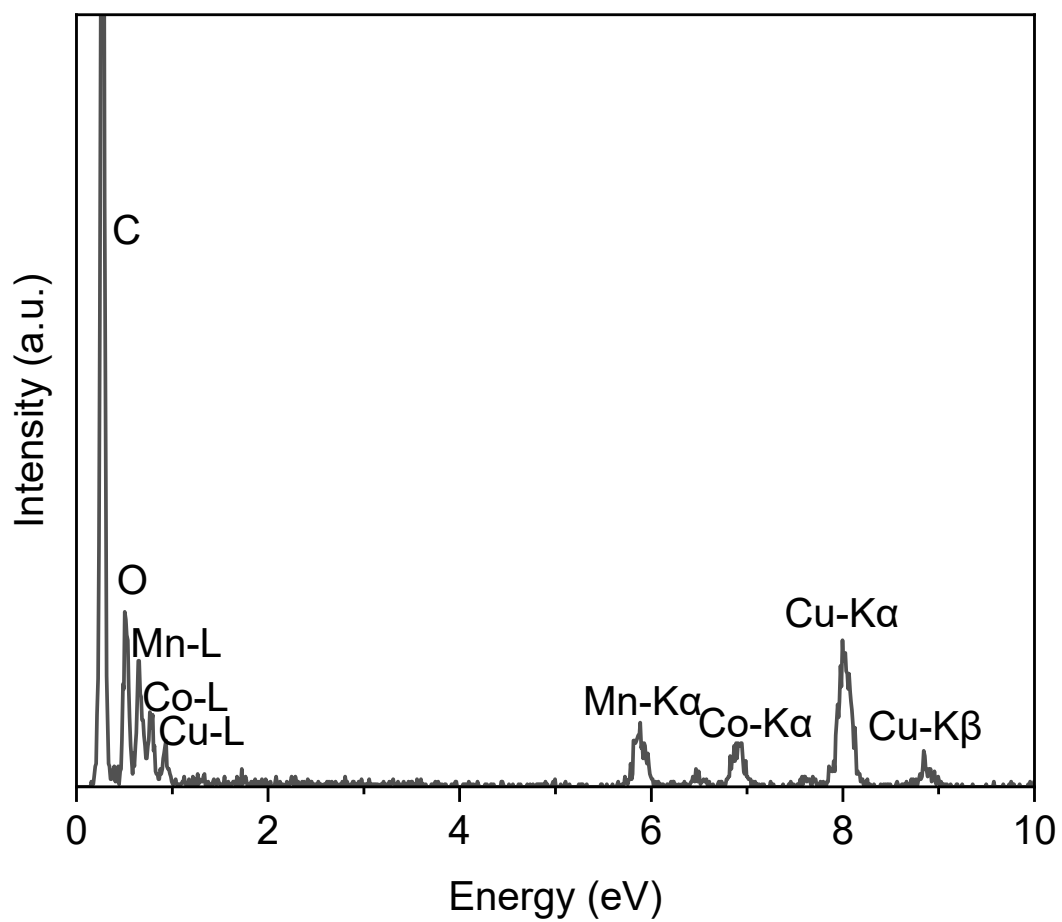


**Figure S9.** EDS elemental spectrum of pristine MCS electrode.

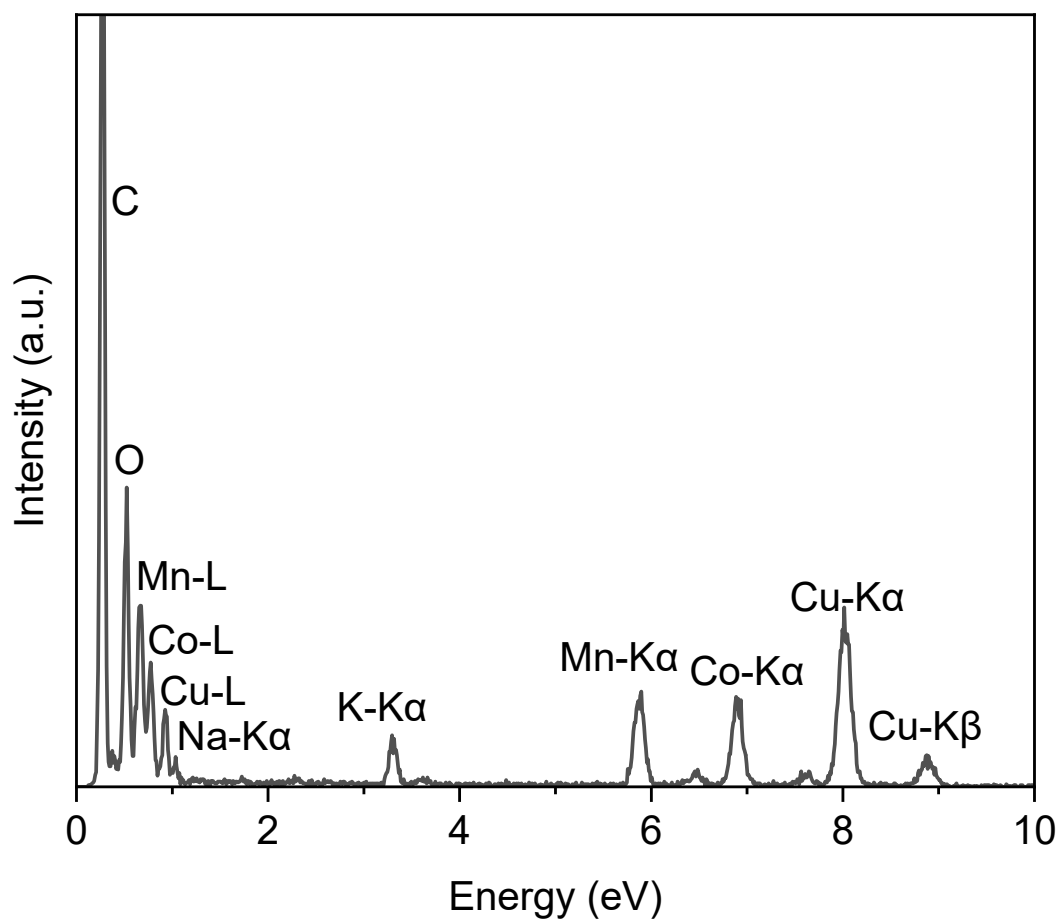


**Figure S10.** EDS elemental spectrum of MCS electrode after durability test.

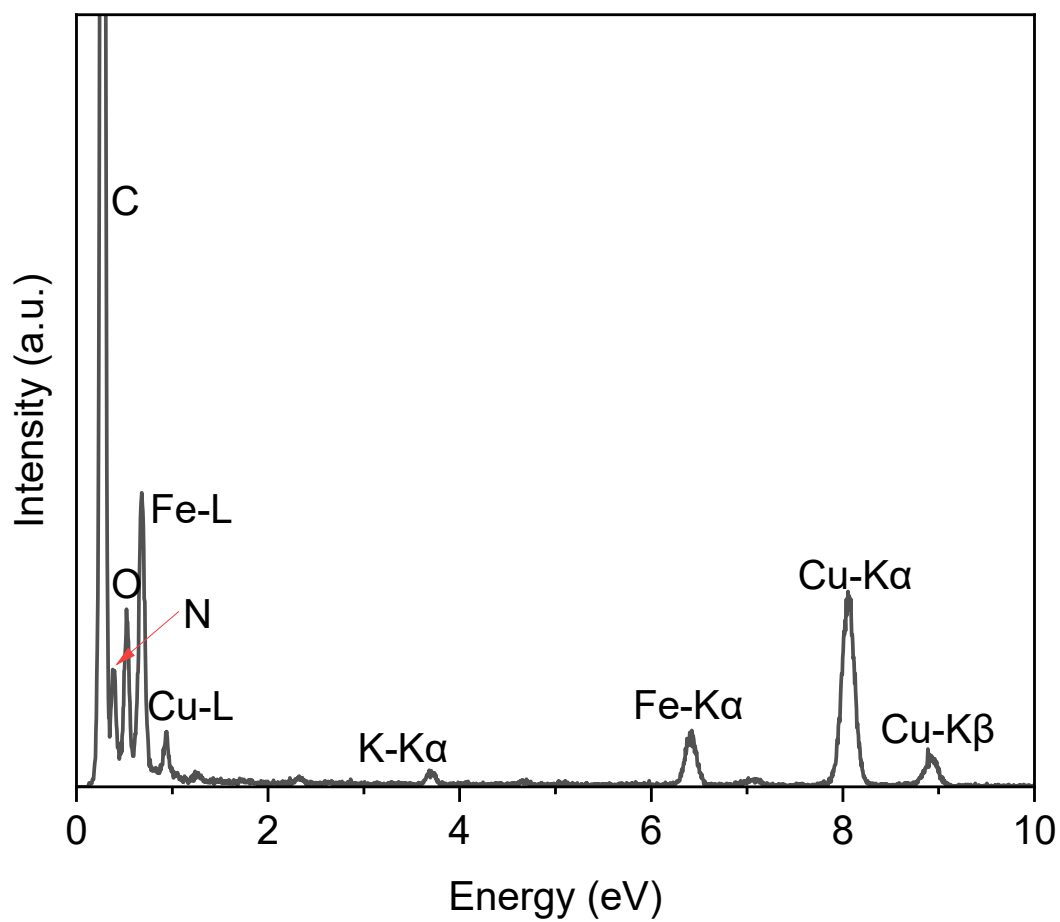


**Figure S11.** EDS elemental spectrum of pristine Fe-N-C electrode.



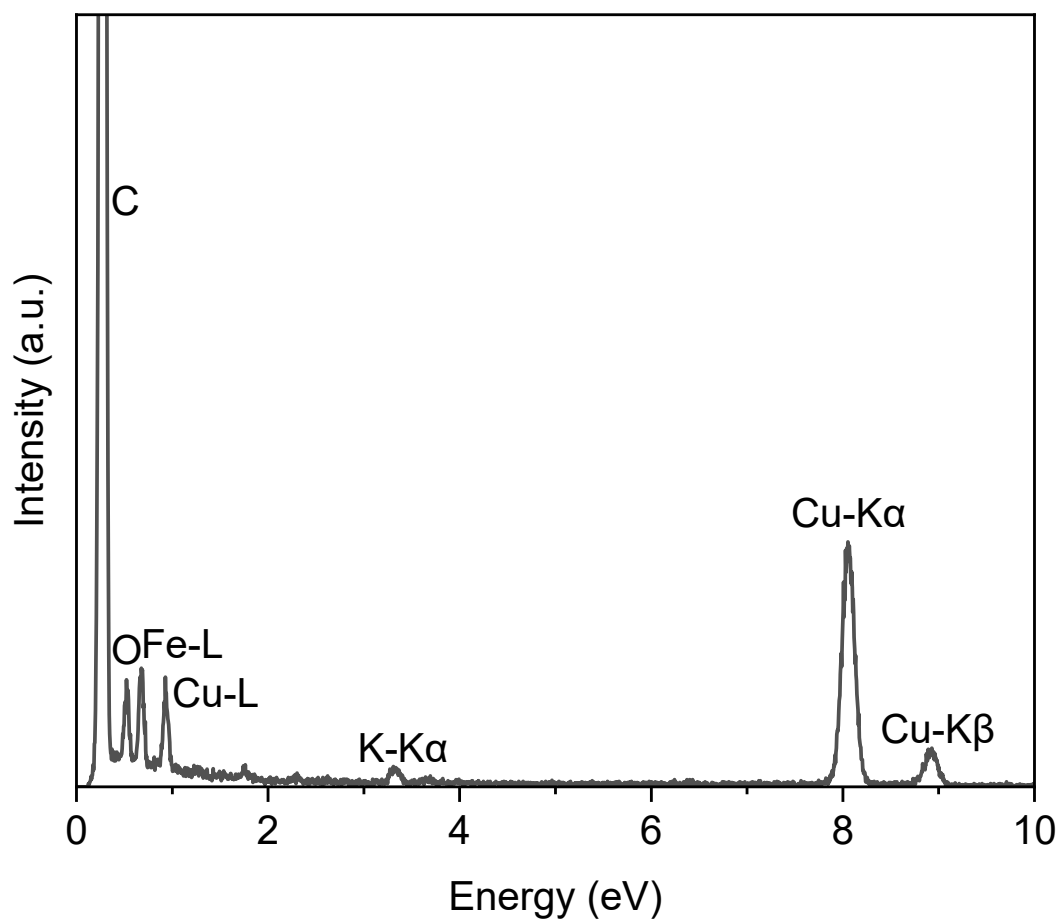


**Figure S12.** EDS elemental spectrum of Fe-N-C electrode after durability test.

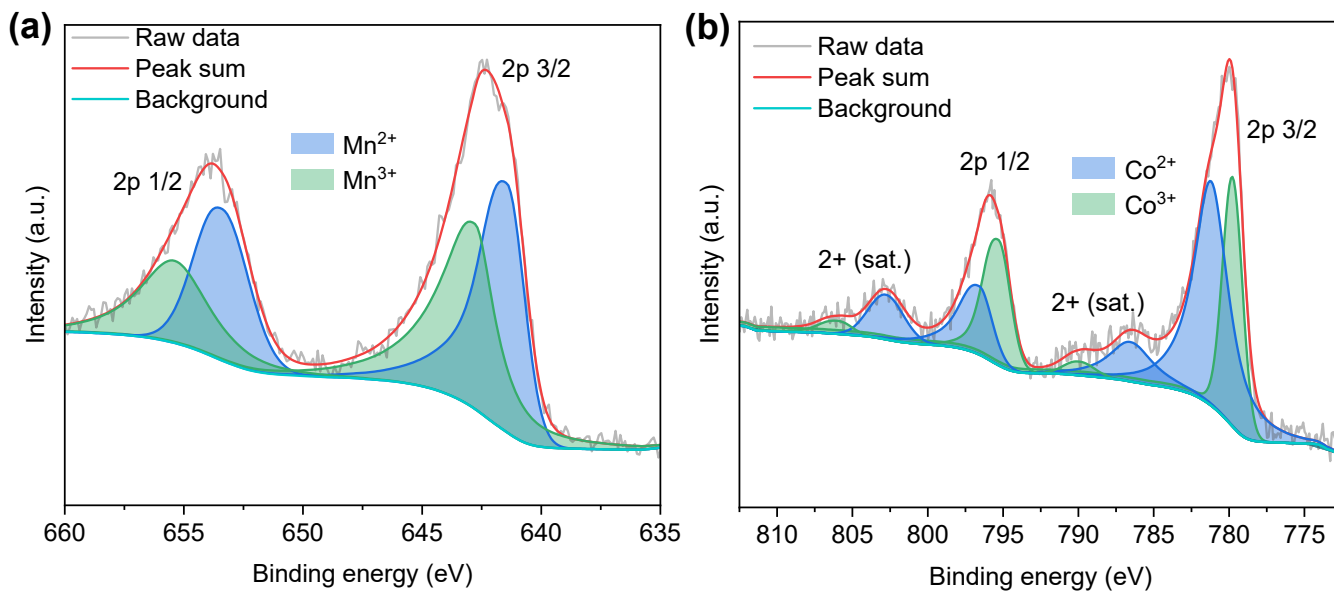


**Figure S13.** XPS high-resolution (a) Mn 2p, and (b) Co 2p spectra of pristine LMCO electrode.

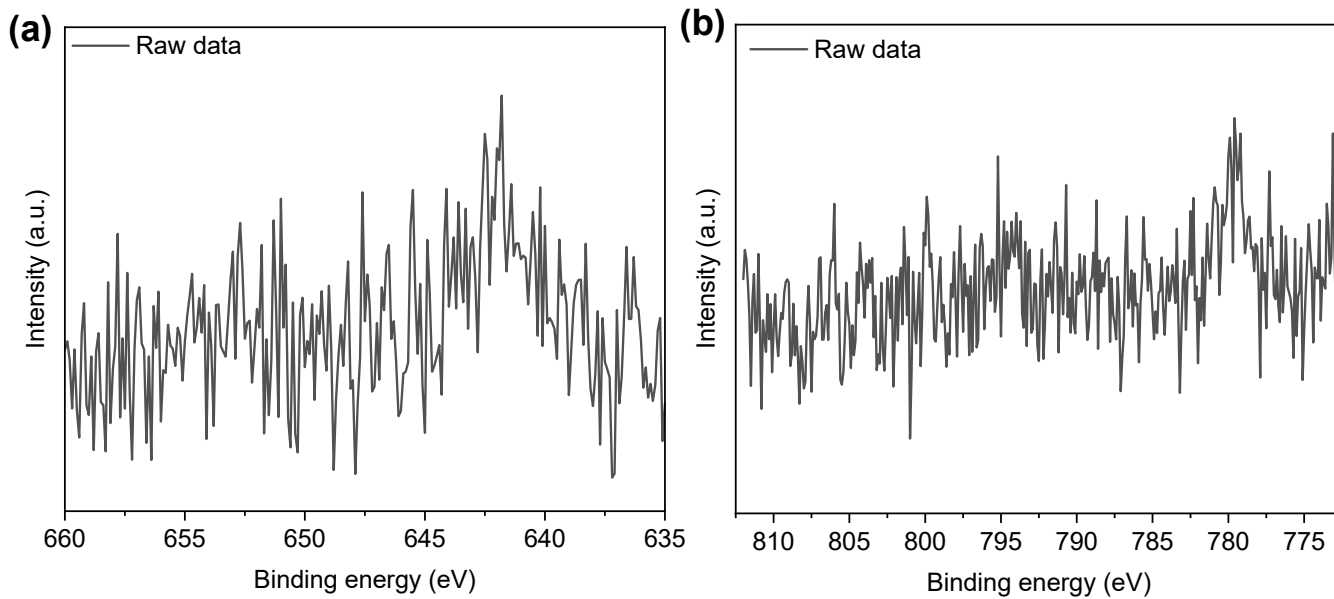


**Figure S14.** XPS high-resolution (a) Mn 2p, and (b) Co 2p spectra of LMCO electrode after durability test.

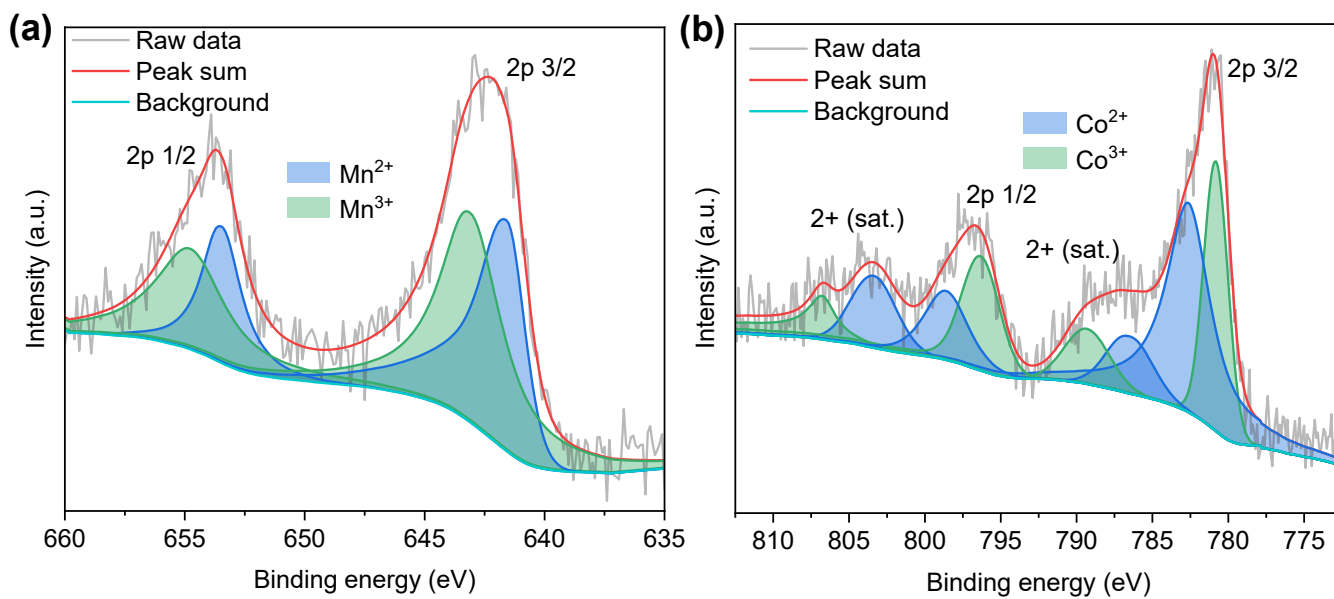


**Figure S15.** XPS high-resolution (a) Mn 2p, and (b) Co 2p spectra of pristine MCS electrode.



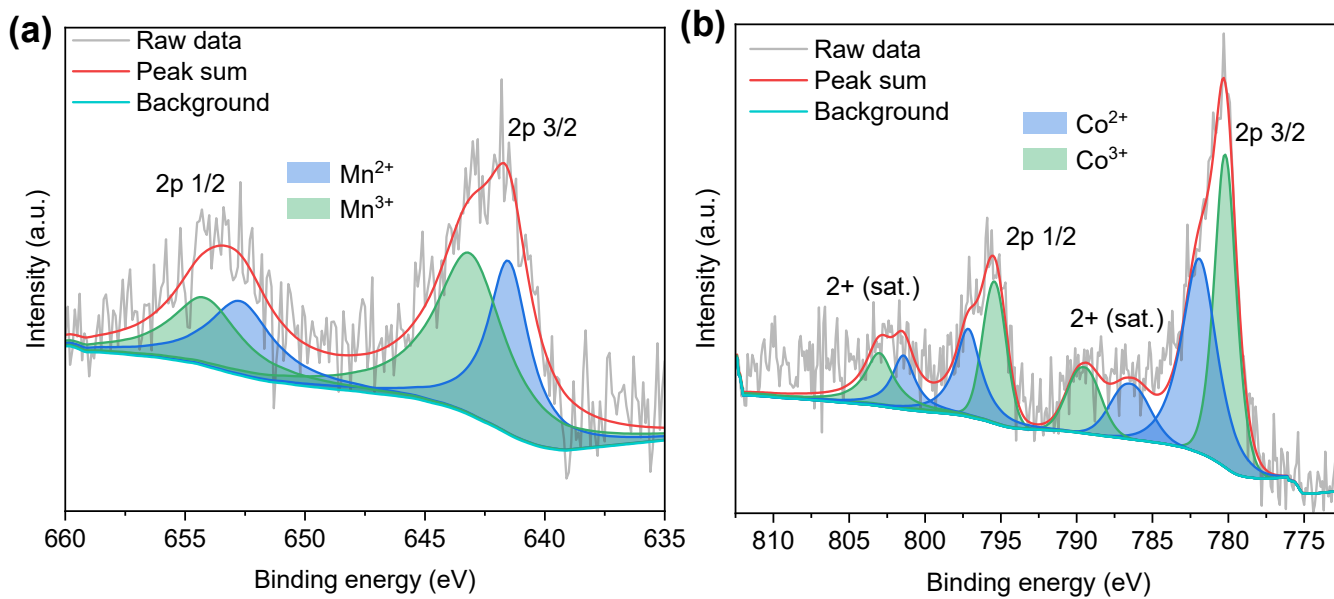


**Figure S16.** XPS high-resolution (a) Mn 2p, and (b) Co 2p spectra of MCS electrode after durability test.

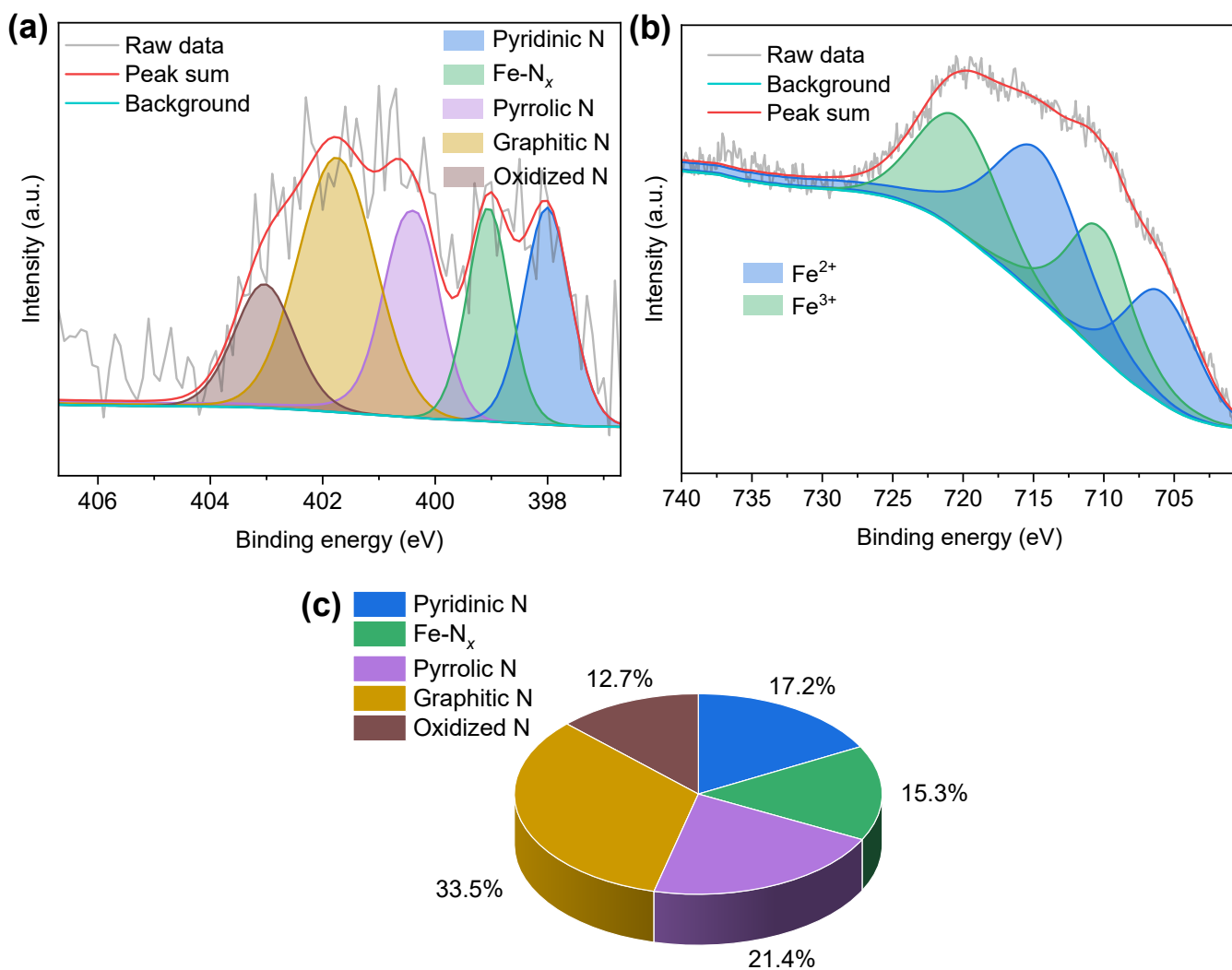


**Figure S17.** XPS high-resolution (a) N 1s, (b) Fe 2p spectra, and (c) comparison of different N species contents of pristine Fe-N-C electrode.

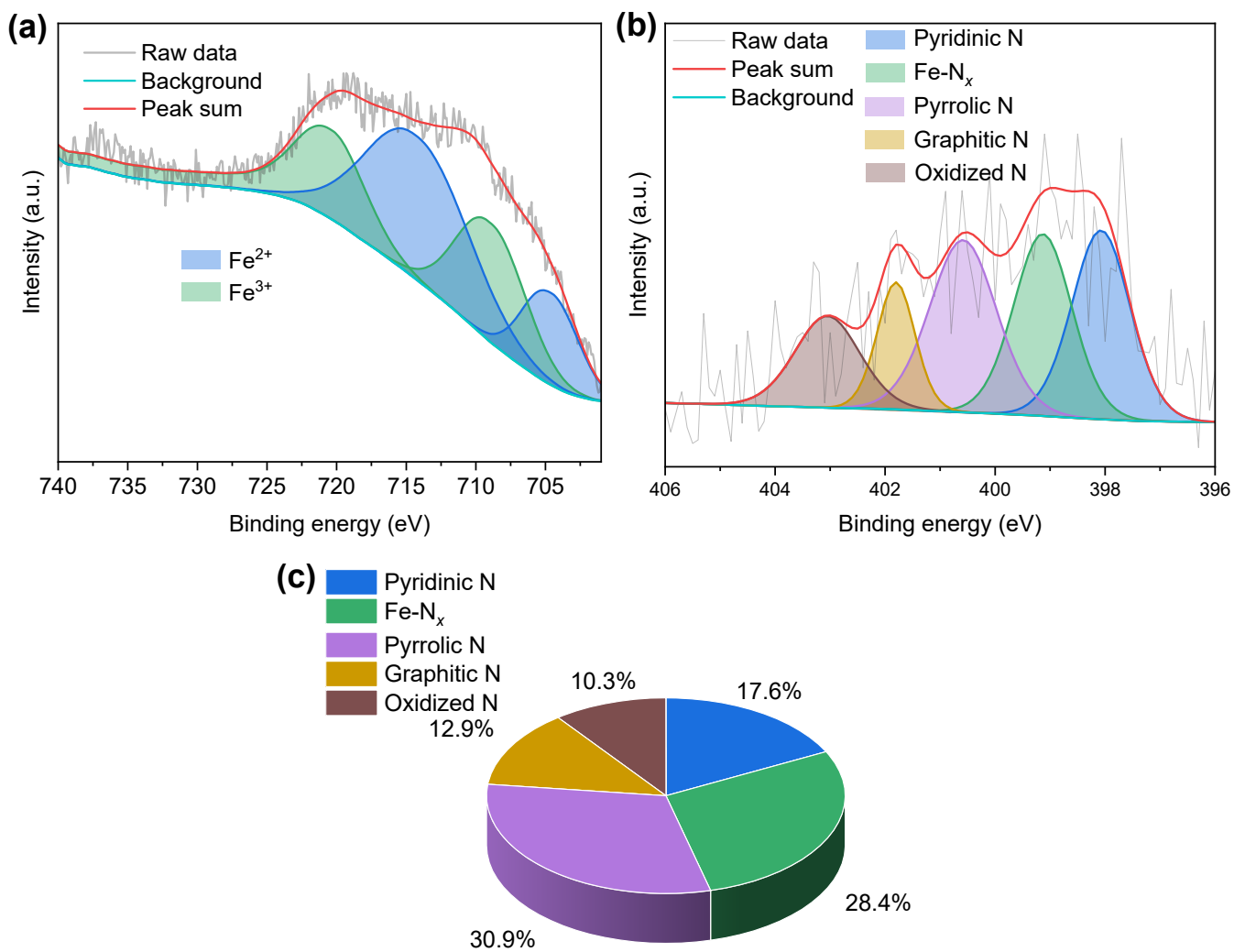


**Figure S18.** XPS high-resolution (a) N 1s, (b) Fe 2p spectra, and (c) comparison of different N species contents of Fe-N-C electrode after durability test.

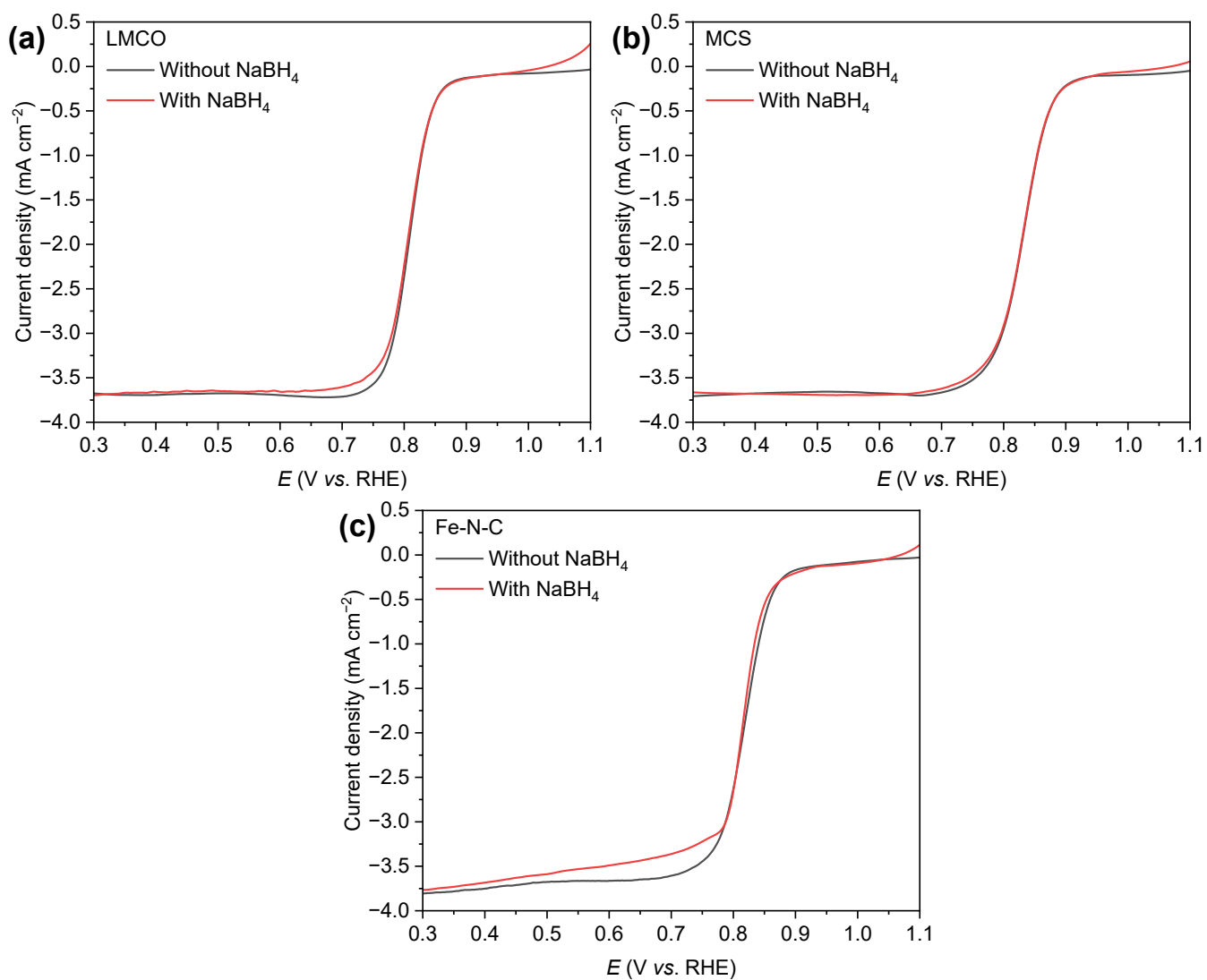


**Figure S19.** ORR polarization curves of (a) LMCO, (b) MCS, and (c) Fe-N-C at 25 °C, 20 mV s<sup>-1</sup>, and 1600 rpm, in O<sub>2</sub>-saturated 1 M KOH solution with or without 10 mM NaBH<sub>4</sub>.



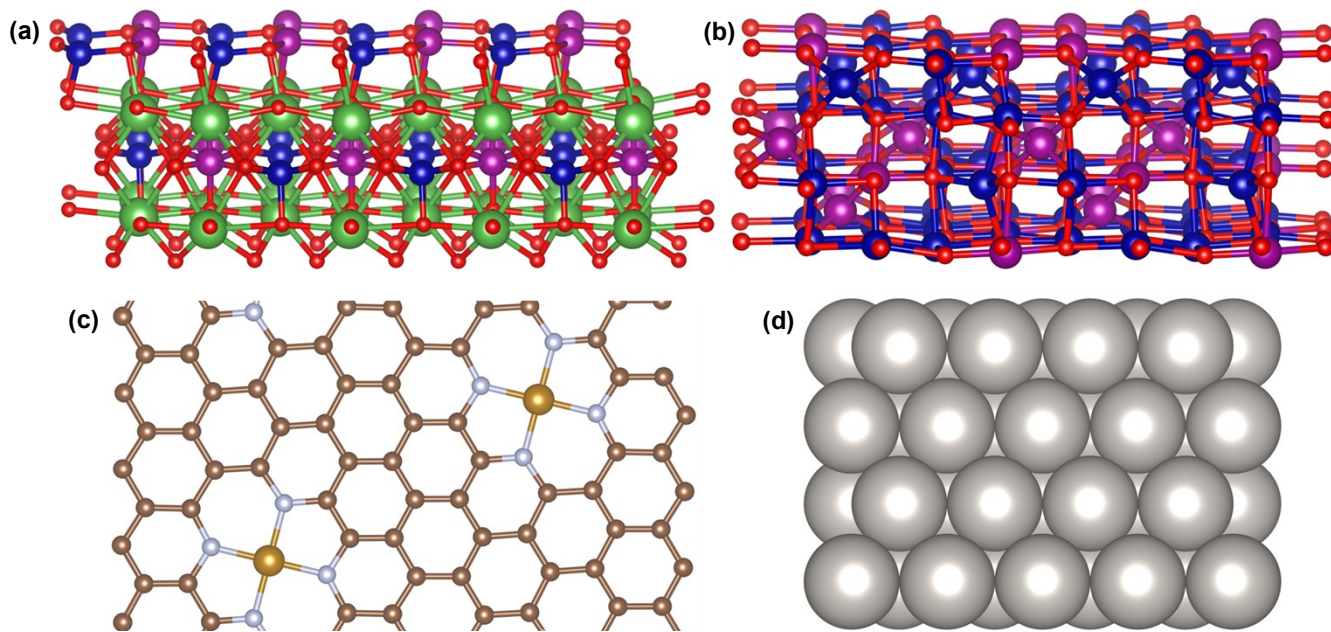


**Figure S20.** DFT optimized structure of (a) LMCO, (b) MCS, (c) Fe-N-C, and (d) Pt.

**Table S1.** Textural properties of the catalysts.

Sample	$S_{\text{BET}}$ ( $\text{m}^2 \text{g}^{-1}$ )	$S_{\text{micro}}$ ( $\text{m}^2 \text{g}^{-1}$ )	$S_{\text{meso}}$ ( $\text{m}^2 \text{g}^{-1}$ )	Total pore volume ( $\text{m}^2 \text{g}^{-1}$ )
LMCO	1451	910	541	2.24
MCS	1538	985	553	2.59
Fe-N-C	734	427	307	0.61

**Table S2.** The comparison of the single cell performance of representative studies.

Anode catalyst	Membrane	Cathode catalyst	Oxidant	Peak power density (mW cm <sup>-2</sup> )	Ref.
Co-W-B	Membraneless	LaNi <sub>0.9</sub> Ru <sub>0.1</sub> O <sub>3</sub> /CNT	Air	500	1
Pd/C + Ni	Nafion <sup>®</sup> 117	Pt/C	H <sub>2</sub> O <sub>2</sub>	630	2
Pd/C + Ni	Nafion <sup>®</sup> 117	Pt/C	H <sub>2</sub> O <sub>2</sub>	890	3
PdNi/C	Nafion <sup>®</sup> 117	Pt/C	H <sub>2</sub> O <sub>2</sub>	630	4
CoO	Nafion <sup>®</sup> 211	RuO <sub>2</sub>	H <sub>2</sub> O <sub>2</sub>	425	5
Pd/C + Ni	Nafion <sup>®</sup> 117	Pt/C	H <sub>2</sub> O <sub>2</sub>	580	6
Pt/C	Nafion <sup>®</sup> 117	Pt/C	H <sub>2</sub> O <sub>2</sub>	800	7
PteAu/C	Nafion <sup>®</sup> 117	Pt/C	H <sub>2</sub> O <sub>2</sub>	345	8
Ni+Pd/C	Nafion <sup>®</sup>	Pt/C	H <sub>2</sub> O <sub>2</sub>	590	9
AB <sub>5</sub> alloy	Nafion <sup>®</sup> 117	Pt/C	H <sub>2</sub> O <sub>2</sub>	352	10
AB <sub>5</sub> alloy	Nafion <sup>®</sup> 117	Pd/C	H <sub>2</sub> O <sub>2</sub>	589	11
Ni particle on Ni felt	Nafion <sup>®</sup> 117	Pt/C	H <sub>2</sub> O <sub>2</sub>	446	12
Pd–Ni/N-rGO	Nafion <sup>®</sup> 117	Pt/C	H <sub>2</sub> O <sub>2</sub>	353.84	13
Core (Ni)-Shell (Pd)/rGP1	Nafion <sup>®</sup>	Pt/C	H <sub>2</sub> O <sub>2</sub>	339.1	14
Pt/[TaOPO <sub>4</sub> /VC]	Nafion <sup>®</sup> 117	Pt/C	H <sub>2</sub> O <sub>2</sub>	360	15
nanoporous Au	Nafion <sup>®</sup> 212	nanoporous Au	H <sub>2</sub> O <sub>2</sub>	390	16
Au	Nafion <sup>®</sup>	Pd	H <sub>2</sub> O <sub>2</sub>	680	17
Au	Nafion <sup>®</sup>	Pd	H <sub>2</sub> O <sub>2</sub>	680	17
Au	Nafion <sup>®</sup>	Pd	H <sub>2</sub> O <sub>2</sub>	1500	18
Zn foil	Nafion <sup>®</sup> 117	Pt	H <sub>2</sub> O <sub>2</sub>	528	19
Ni + Pt/C	Nafion <sup>®</sup> 212	Pd	H <sub>2</sub> O <sub>2</sub>	665	20
Ni + Pd/C	Polymer electrolyte membrane	Pt/C	H <sub>2</sub> O <sub>2</sub>	810	21
Pt–Ru	Nafion <sup>®</sup> 115	Pd–Ir	H <sub>2</sub> O <sub>2</sub>	345	22
Pd/C	A-006 (AEM)	Fe–Co	O <sub>2</sub>	890	23
Ni/C	Nafion <sup>®</sup> 212	Hypermec <sup>™</sup> K14	O <sub>2</sub>	460	24
Pd/C + Ni	triphosphate chitosan hydrogel	Pt/C	O <sub>2</sub>	685	25
Pd/C + Ni	cross-linked chitosan	Pt/C	O <sub>2</sub>	450	26
Ni-based thin film	chitosan hydrogel (AEM)	Pt/C	O <sub>2</sub>	429	27
Co–pyrrole/MPC	Nafion <sup>®</sup> 112	Pt/C	O <sub>2</sub>	325	28
Pd decorated Ni–Co/C	AEM	Fe–Co/C	O <sub>2</sub>	761	29

CoO	polymer fiber membrane	LaNiO <sub>3</sub>	O <sub>2</sub>	663	30
Co(OH) <sub>2</sub> -PPy- BP	Nafion <sup>®</sup> 212	CoO Nanorods/C	O <sub>2</sub>	410	31
Co(OH) <sub>2</sub> -PPy- BP	Co-PVA & PVA bilayer (AEM)	Co(OH) <sub>2</sub> -PPy-BP	O <sub>2</sub>	327	32
Co(OH) <sub>2</sub> -PPy- BP	AEM	Co(OH) <sub>2</sub> -PPy-BP	O <sub>2</sub>	500	33
NiFe-2	Nafion <sup>®</sup> 117	Pt/C	H <sub>2</sub> O <sub>2</sub>	540	34
Ni@NiP	Nafion <sup>®</sup> 117	Pt/C	H <sub>2</sub> O <sub>2</sub>	474	35
Pt/C	Alkymer <sup>®</sup>	Mn-Co Spinel	O <sub>2</sub>	1518	This work

---

## References

- 1 S. Li, X. Yang, H. Zhu, X. Wei and Y. Liu, *Int. J. Hydrog. Energy*, 2013, **38**, 2884–2888.
- 2 Z. Wang, J. Parrondo, C. He, S. Sankarasubramanian and V. Ramani, *Nat. Energy*, 2019, **4**, 281–289.
- 3 Z. Wang, S. Sankarasubramanian and V. Ramani, *Cell Rep. Phys. Sci.*, 2020, **1**, 100084.
- 4 S. Saha, P. Gayen, Z. Wang, R. J. Dixit, K. Sharma, S. Basu and V. K. Ramani, *ACS Catal.*, 2021, **11**, 8417–8430.
- 5 X. Yang, X. Wei, C. Liu and Y. Liu, *Mater. Chem. Phys.*, 2014, **145**, 269–273.
- 6 Z. Wang, M. Mandal, S. Sankarasubramanian, G. Huang, P. A. Kohl and V. K. Ramani, *ACS Appl. Energy Mater.*, 2020, **3**, 4449–4456.
- 7 N. Luo, G. H. Miley, J. Mather, R. Burton, G. Hawkins, R. Gimlin, J. Rusek, T. I. Valdez and S. R. Narayanan, *AIP Conf. Proc.*, 2006, **813**, 209–221.
- 8 O. Okur, E. Alper and A. Almansoori, *Energy*, 2014, **67**, 97–105.
- 9 Y. Ko, L. Lombardo, M. Li, T. H. M. Pham, H. Yang and A. Züttel, *Adv. Energy Mater.*, 2022, **12**, 2103539.
- 10 R. K. Raman, N. A. Choudhury and A. K. Shukla, *Electrochem. Solid-State Lett.*, 2004, **7**, A488.
- 11 N. A. Choudhury, J. Ma, Y. Sahai and R. G. Buchheit, *J. Power Sources*, 2011, **196**, 5817–5822.
- 12 G. Braesch, Z. Wang, S. Sankarasubramanian, A. G. Oshchepkov, A. Bonnefont, E. R. Savinova, V. Ramani and M. Chatenet, *J. Mater. Chem. A*, 2020, **8**, 20543–20552.
- 13 M. G. Hosseini, V. Daneshvari-Esfahlan, S. Wolf and V. Hacker, *ACS Appl. Energy Mater.*, 2021, **4**, 6025–6039.
- 14 R. Mahmoodi, M. G. Hosseini and H. Rasouli, *Appl. Catal., B*, 2019, **251**, 37–48.
- 15 R. M. E. Hjelm, Y. Garsany, C. Lafforgue, M. Chatenet and K. Swider-Lyons, *ECS Trans.*, 2018, **86**, 659.
- 16 W. Jin, J. Liu, Y. Wang, Y. Yao, J. Gu and Z. Zou, *Int. J. Hydrog. Energy*, 2013, **38**, 10992–10997.
- 17 L. Gu, N. Luo and G. H. Miley, *J. Power Sources*, 2007, **173**, 77–85.
- 18 N. Luo, G. H. Miley, K.-J. Kim, R. Burton and X. Huang, *J. Power Sources*, 2008, **185**, 685–690.
- 19 D. M. F. Santos and C. a. C. Sequeira, *J. Electrochem. Soc.*, 2009, **157**, B13.
- 20 J. Ma, Y. Sahai and R. G. Buchheit, *J. Power Sources*, 2010, **195**, 4709–4713.
- 21 N. A. Choudhury, J. Ma and Y. Sahai, *J. Power Sources*, 2012, **210**, 358–365.
- 22 D. Cao, D. Chen, J. Lan and G. Wang, *J. Power Sources*, 2009, **190**, 346–350.
- 23 M. Zhiani, I. Mohammadi and N. Salehi, *RSC Adv.*, 2015, **5**, 23635–23645.
- 24 G. Braesch, A. G. Oshchepkov, A. Bonnefont, F. Asonkeng, T. Maurer, G. Maranzana, E. R. Savinova and M. Chatenet, *ChemElectroChem*, 2020, **7**, 1789–1799.
- 25 J. Ma, Y. Sahai and R. G. Buchheit, *J. Power Sources*, 2012, **202**, 18–27.
- 26 J. Ma, N. A. Choudhury, Y. Sahai and R. G. Buchheit, *J. Power Sources*, 2011, **196**, 8257–8264.
- 27 J. Ma and Y. Sahai, *ECS Electrochem. Lett.*, 2012, **1**, F41.
- 28 Y. Chen, S. Wang and Z. Li, *RSC Adv.*, 2020, **10**, 29119–29127.
- 29 M. Zhiani and I. Mohammadi, *Fuel*, 2016, **166**, 517–525.
- 30 X. Yang, Y. Liu, S. Li, X. Wei, L. Wang and Y. Chen, *Sci. Rep.*, 2012, **2**, 567.
- 31 J. Jia, X. Li, H. Qin, Y. He, H. Ni and H. Chi, *J. Alloy. Compd.*, , DOI:10.1016/j.jallcom.2019.153065.
- 32 X. Li, H. Chen, W. Chu, H. Qin, W. Zhang, H. Ni, H. Chi, Y. He, Y. S. Chu, J. Hu and J. Liu, *ACS*

*Appl. Mater. Inter.*, 2020, **12**, 27184–27189.

33 J. Wei, X. Han, X. Li, H. Qin, H. Yin, W. Zhang, H. Ni and X. Wang, *RSC Adv.*, 2022, **12**, 28707–28711.

34 Y. Yang, X. Zhu, C. Yi, H. Yang, X. Hou, X. Liao, C. Chen, D. Yu and X. Zhou, *Chem. Eng. J.*, 2023, **472**, 145097.

35 B. Hu, Y. Xie, Y. Yang, J. Meng, J. Cai, C. Chen, D. Yu and X. Zhou, *Appl. Catal., B*, 2023, **324**, 122257.